



The effect of MoO₃ substitution for B₂O₃ on the structural and optical properties of bismuth borate glass

I. Kashif¹ · A. Ratep²

Received: 3 December 2021 / Revised: 5 April 2022 / Accepted: 12 June 2022 / Published online: 21 June 2022
© The Author(s) under exclusive licence to Australian Ceramic Society 2022

Abstract

Fifty Bi₂O₃–(50–*x*) B₂O₃–*x*MoO₃ glasses with *x* = 0, 5, 10, 15, and 20 are made using the melt-quenching procedure (mol%). The structural and physical properties of the produced glass samples were investigated using X-ray diffraction (XRD), infrared (FTIR), and optical absorption (UV/Vis/NIR) spectroscopy. In vitreous compositions including MoO₃ up to 15 mol% and semi-crystallized samples containing 20 mol%, the environment of cations was examined. When the sample is poured into the air, the Bi₂MoO₆ crystalline phase forms, and the crystalline intensity increases. The isolated MoO₄ presence in structural groups in the glass network can be seen in FTIR data. The thermal stability of glass samples containing 5 and 10 mol% MoO₃ is higher than that of other samples.

Keywords Bismuth molybdenum borate glass · XRD · DTA · FTIR · Optical properties

Introduction

Bismuth borate glass is a promising candidate for applications such as infrared transmission components, ultrafast optical switches, and photonic devices, as well as a variety of other applications such as magneto-optical current transducer (MOCT) for high voltage current systems, optical rotators, and isolates, or circulators, switches, and polarimeters [1–4].

Boron oxide (B₂O₃) is the most frequent glass-forming, with trigonal BO₃ and tetrahedral BO₄ units entering the structure. This material has good transparency, chemical durability, and thermal stability and is created at a low melting temperature [5]. Electrical, optical, and luminescent capabilities are all present in borate glass [6]. The addition of transition metal to borate glass increases their optical properties, which are due to the transition metal's varied oxidation states [7]. Microelectronics, optical glasses, solid-state lasers [8, 9], and semiconductor characteristics [10] all benefit from it.

Depending on the chemical content and composition, the addition of MoO₃ in alkali borate glass [6] produces two oxidation states: Mo⁵⁺ and Mo⁶⁺. The polarizability of oxygen around magnetic ions, the concentration of NBOs, and the coordination number were all altered by the ratio of different oxidation states of MoO₃.

Because it is employed in thermal, mechanical, and optical devices, heavy metal oxide glass receives greater attention. Bi₂O₃ exists in the valance states Bi⁶⁺ and Bi³⁺, which have low field strength and high polarizability [11].

Bismuth glass also has other benefits, including third-order nonlinear optics, a high refractive index, and an infrared cut-off. Because of its piezoelectric, ferroelectric, and pyroelectric capabilities, the glass with Bi and B is used in more applications.

Kh. S. Shaaban [10] studied the structural, thermal, mechanical, and optical properties of the bismuth borosilicate glass system when Bi₂O₃ was replaced with MoO₃ and discovered that the properties of study glass samples are more susceptible to the MoO₃ concentration. Alternatively, the bond strength, ultrasonic velocity, elastic moduli, and thermal stability all increase.

E. S. Moustafa et al. [12] investigated the structural and optical properties of lithium borobismuthate glasses and discovered that as the structure closes due to the transformation of BO₃ to BO₄, the density and molar volume decrease at the expense of Bi₂O₃ as the structure becomes closed,

✉ I. Kashif
ismailkashif52@yahoo.com

¹ Department of Physics, Faculty of Science, Al-Azhar University, Cairo, Nasr City, Egypt

² Physics Department, Faculty of Women for Arts, Science & Education, Ain Shams University, Cairo, Heliopolis, Egypt

as confirmed by FTIR measurements. They discovered that the bond strength of B–O and the reduction in the oxygen environment of bismuth cations were linked to changes in optical characteristics.

Anu Bajaj et al. [13] investigated bismuth borate glass and discovered that increasing the Bi_2O_3 content increased the molar volume while decreasing the glass transition temperature. A glass sample with 50 mol% Bi_2O_3 has the most tetra-boron-coordinated atoms (N_4).

The goal of this research is to see how adding B_2O_3 , a heavy metal, and MoO_3 , a transition metal, affects the results. Simultaneously, investigate the implications of substituting transition metals for heavy metals on structural, thermal, and optical properties.

Experimental

As starting materials, reagent grades H_3BO_3 , Bi_2O_3 , and MoO_3 are used to make glasses with the composition 50 Bi_2O_3 –(50– x) B_2O_3 – x MoO_3 mol%, where $x = 0, 5, 10, 15$, and 20 mol%, and the samples are kept at roughly 300 °C for half an hour to de-carbonize the carbonate.

The temperature was then raised to 1000 °C and held for 1 h. At normal temperature, the molten liquid spilled between two copper plates and a few droplets in the air. The glassy and crystalline character of the samples was investigated and validated using a Philips Analytical System (XRD) of type PW3710 with a Cu tube anode of wavelengths $K_{\alpha 1} = 1.54060$ and $K_{\alpha 2} = 1.54439$. The generator current was 30 mA, and the generator tension was 40 kV. The starting angle (θ) was 10°, and the ending angle was 70°.

In this study, absorption spectra in the range of 400–4000 cm^{-1} were analyzed using an infrared spectrometer (FTIR 4100; JASCO, Japan).

The produced samples were subjected to differential thermal analysis (DTA) in the temperature range of 30 to 1200 °C at a heating rate of 30 °C/min using Al_2O_3 powder as a reference material (Shimadzu DTA-50analyzer).

The density is calculated using the Archimedes method and the following equation:

$$\rho(\text{gcm}^{-3}) = [a(a - b)^{-1}] (\text{density of the Toluene})$$

where a represents the sample weight in air and b represents the sample weight in toluene.

A computerized spectrophotometer was used to measure the optical transmission spectra in the region of 190 to 2500 nm (JASCO, V-570).

X-ray photoelectron spectroscopy (XPS) studies were performed with an ESCALAB 220iXL spectrometer (Fisons Instruments) consisting of two vacuum chambers: the analyzer and the fast entry airlock/preparation chamber. The

powdered samples were fixed on carbon conductive tape (Pelco International) at the top of the sample holder and transferred into the ultra-high vacuum. The X-ray source was monochromatic-focused Al K α radiation (1486.6 eV) with an input power of 150 W. The emerging charge of the sample equalized with the installed charge compensation. The final peak position was determined using the C 1 s peak (shifted to 285.0 eV) corresponding to absorb carbon species. The XPS measurements were carried out at the constant pass energy of 25 eV.

Results and discussion

Structural properties

X-Ray diffraction (XRD)

The XRD for bismuth borate glass samples containing molybdenum oxide from 0 to 20 mol% is shown in Fig. 1a. It was observed that samples containing molybdenum oxide up to 15 mol% MoO_3 are amorphous in nature (Fig. 1a). However, a sample having 20 mol% MoO_3 is both un-crystalline and crystalline.

The sample of 20 mol% MoO_3 was poured between two copper plates or poured into the air contained 20 mol% MoO_3 , according to the analysis.

The creation of the crystalline Bi_2MoO_6 phase is more intense in the sample poured into the air than in the sample poured between two copper plates, according to the X-ray diffraction patterns of the sample containing 20 mol%. Aurivillius oxides [14], which have perovskite-like layer structures, photocatalytic activity under visible light irradiation, high optical absorption efficiency, and low photo-induced recombination efficiency, are photosensitive to this phase. And the crystalline phase separated in a sample containing 20 mol% MoO_3 compared with XRD patterns of Bi_2MoO_6 , B_2O_3 , Bi_2O_3 , and MoO_3 crystalline phases as shown in Fig. 1b.

FTIR

The infrared spectra of glass samples are shown in Fig. 2. The FTIR spectra revealed the structural arrangement of the structural units presents in glass samples with a composition of 50 Bi_2O_3 –(50– x) B_2O_3 – x MoO_3 , where $x = 0.0, 5, 10, 15$, and 20 mol%. For the Bi and B groups, the FTIR provides information on stretching and bending vibration. It reveals three wide zones [7], all of which clearly illustrate the presence of borate groups.

The very first group the asymmetric stretching vibration of B–O bonds of trigonal BO_3 units causes the change from 1500 to 1140 cm^{-1} . (ii) Due to the B–O bond stretching of tetrahedral BO_4 units, the second band was allocated from

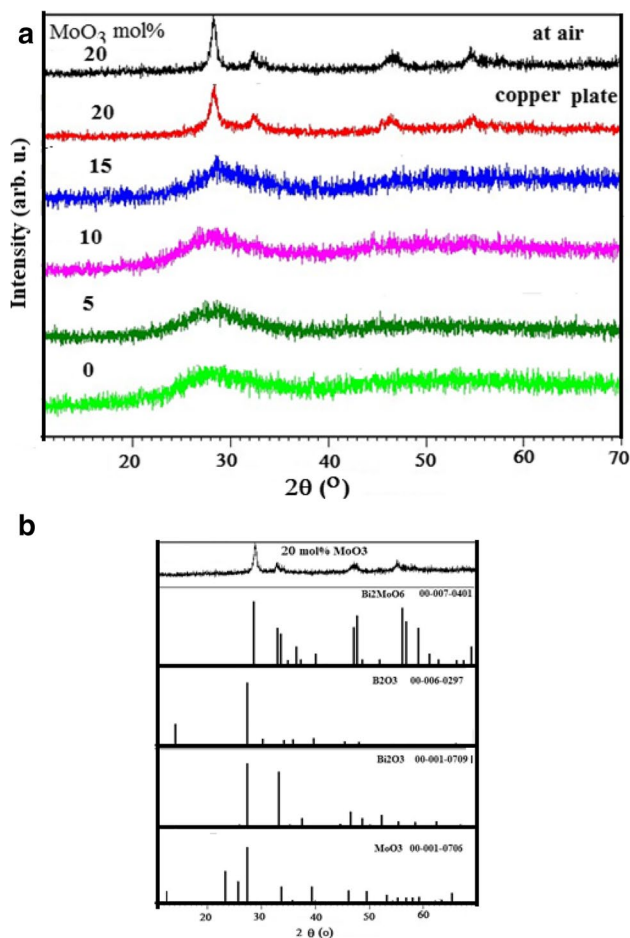
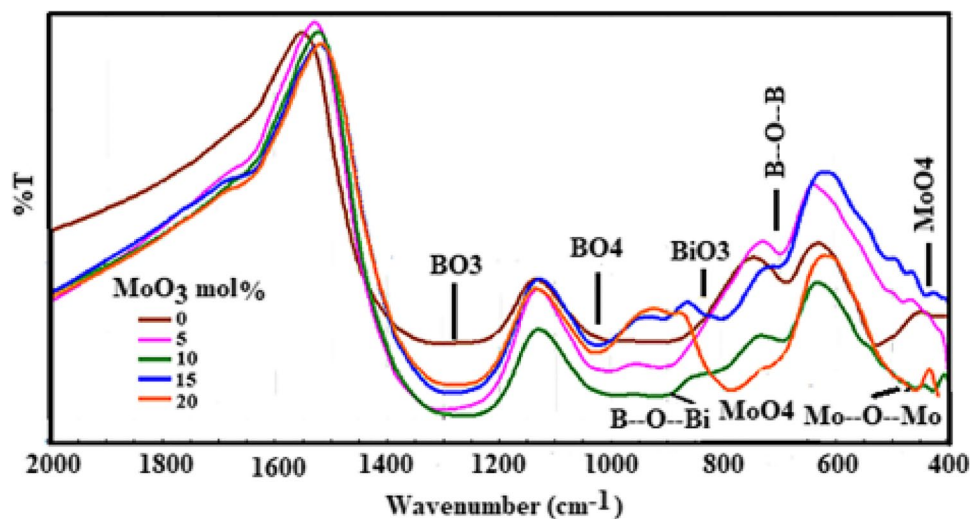


Fig. 1 The XRD for bismuth borate glass samples containing molybdenum oxide from 0 to 20 mol%

1140 to 750 cm⁻¹. (iii) The third band, ranging from 750 to 650 cm⁻¹, is caused by the borate network's B–O–B bending vibrations.

Fig. 2 The infrared spectra of glass samples



Bismuth in borate glass, on the other hand, appears in FTIR spectra as precisely placed bands. There are four infrared active basic vibrations of [BiO₃] pyramidal units: an asymmetric stretching vibration (840 cm⁻¹), a doubly degenerate stretching vibration (540–620 cm⁻¹), an asymmetric bending vibration (470 cm⁻¹), and a doubly degenerate bending vibration (540–620 cm⁻¹) (350 cm⁻¹) [15].

When MoO₃ is added to bismuth borate glass, it forms Mo⁶⁺ and Mo⁵⁺, which act as a former when coupled to four oxygen atoms, generating MoO₄ tetrahedral structural units, and as a modifier when linked to six oxygen atoms, forming MoO₆ octahedral structural units [7].

The emergence of vibration bands around 750–920 cm⁻¹ and 430–410 cm⁻¹ as the concentration of MoO₃ increased was attributed to the presence of isolated MoO₄ structural groups in the glass network [16].

The symmetric and asymmetric Mo–O–Mo vibrations are responsible for the two bands at 450 and 600 cm⁻¹, respectively. As the symmetric stretching vibration of BiO₃ pyramidal units [7] overlapped with the Mo–O–Mo band and as the BiO₆ structure units [5] overlapped with the MoO₄ band [6], the increase in MoO₃ led to the appearance of Bi in the former structure. On the other hand, as Mo increases, the coupling between B and Bi in the 968–1025 cm⁻¹ band appears to extend the B–O–Bi vibrations [5].

However, no Mo–O–B bonds were found. The significant tendency for liquid phase separation in compositions comprising B₂O₃ and MoO₃ concurrently is due to the absence of connectivity between MoO_n and BO_n polyhedral in the amorphous network. It also said that at MoO₃ concentrations less than 50 mol%, there is no chance of the MoO₆ forming.

XPS measurements

Molybdenum can exist in the glass with four valences (Mo³⁺, Mo⁴⁺, Mo⁵⁺, and Mo⁶⁺) that result from the loss of two electrons from the 5 s and one or two of their 5d electrons.

In order to identify the valence state of Mo ions in the glass samples under study, high-resolution XPS spectra for the Mo 3d core level were measured, and the Mo 3d spin–orbit doublet spectra for the glass sample containing 15 mol% MoO₃ are shown in Fig. 3. For the glass sample, the observed two peaks changed within the BEs range 231.84 eV to 232.4 eV and 234.9 eV to 235.66 eV are assigned to the binding energies (BEs) of Mo 3d_{5/2} and Mo 3d_{3/2} (spin–orbit components) of Mo⁶⁺ ions, respectively [17]. The DE noticed between the Mo 3d_{5/2} and Mo 3d_{3/2} peaks is changed within the range 3.06 eV to 3.22 eV for all the glass compositions. Since no peaks are observed at BEs 230 eV (for Mo⁵⁺ state) and 229 eV (for Mo⁴⁺ state) [18, 19] in any of the Mo 3d spectra of glass samples, we assume that there are no Mo⁵⁺ and Mo⁴⁺. Oxidation states are present in our glasses, as the shape of the Mo 3d_{5/2} peak indicates that most Mo presents in a +6 charge state. Thus, the analyses of the Mo 3d spectra confirm the existence of Mo ions in the 6+ oxidation states for all the glass compositions from the XPS measurements.

Physical parameters

The density and molar volume calculations show the variance that occurs in the structural unit. The density overview is explained by the packing between the ions and ionic groups in the structure. [20]

The following formula is used to compute theoretical density ρ_{th} :

$$\rho_{th} = \sum x_i \rho_x$$

Table 1 summarizes the experimental and theoretical densities, where x_i is the molar proportion of oxide and ρ_x is

the density of oxide. There is a small variation between the computed and experimental values that represent the exact measures, as shown in Table 1.

The molar volume, density, and equivalent crystalline volume as a function of molybdenum concentration are shown in Fig. 4. Figure 4 shows that density rises as the amount of MoO₃ (which has a higher molecular weight than B₂O₃) increases. The addition of MoO₃ to the mixture transforms symmetric BO₃ triangles to BO₄ tetrahedral or asymmetric BO₄ triangles in terms of structural units.

BO₄ tetrahedral and asymmetric BO₃ triangles are significantly denser than symmetric BO₃ triangles [9]. According to the relationships [21, 22], the average boron–boron separation $\langle d_{B-B} \rangle$ was determined.

$$\langle d_{B-B} \rangle = \left(\frac{V_m^B}{N} \right)^{1/3}$$

where V_m^B is the volume containing 1 mol of boron atoms within the given glass structure, and $V_m^B = \frac{V_m}{2(1-x_n)}$, x_n is the B₂O₃ molar proportion, and N is the Avogadro's number.

The estimated numbers in Table 1 show that when MoO₃ increases, the values that support the assumption of an increase in glass sample density diminish.

And the molar volume V_m was determined using the following relation [23]:

$$V_m = \sum \frac{x_i M_i}{\rho}$$

where ρ is the sample density, x_i is the molar fraction, and M_i is the molecular weight of all chemical components. Table 1 lists the density values that were collected. Increases in MoO₃ cause a decrease in BO₄ concentration, the development of a new link between B and Bi, and the formation

Fig. 3 Mo 3d core-level spectra for the glass sample containing 20 mol% MoO₃

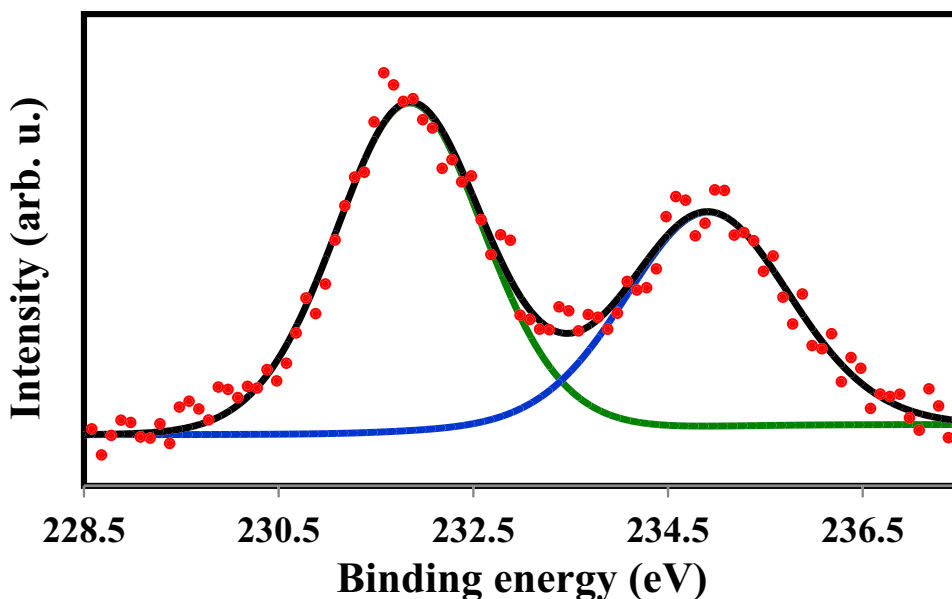


Table 1 Density, molar volume, equivalent crystalline volume, transition temperature T_g , T_c , and T_m , values of glass-forming ability K_{gl}, ΔT , Hruby parameter, and the values of the average boron–boron separation

Conc MoO ₃	ρ Th. (gm/cm ³)	M. V Th. (cm ³ /mol)	ρ exp. (gm/cm ³)	M. V exp. (cm ³ /mol)	V _c (cm ³ /mol)	dB-B 10–8 cm	T_g °C	T_c °C	T_m °C	$\Delta T = T_c - T_g$ °C	$T_{rg} = T_g / T_m$	HR
0	5.68	47.14	5.78	46.33	40.32	3.60	463	512	575	49	0.8	0.78
5	5.79	46.87	5.76	47.13	40.43	3.49	451	515	590	64	0.76	0.85
10	5.9	46.62	5.86	46.96	40.56	3.39	435	507	594	72	0.73	0.82
15	6.01	46.37	5.93	47.04	40.68	3.30	427	465	655	38	0.65	0.2
20	6.12	46.12	6.08	46.49	40.80	3.22	—	—	719	—	—	—

of isolated MO₄ groups, all of which enhance the sample's smallness.

The equivalent crystalline volume (V_c) computed by [23] and given in Table 1 determines whether the sample will become a crystalline or amorphous material:

$$V_c = \sum x_i V_i$$

where V_i is the molar volume of the oxide component in the crystalline phase.

Figure 4 shows that the molar volume (V_i) is greater than the crystalline volume (V_c), indicating the presence of surplus structural volume in these samples and indicating that they are amorphous in nature. The crystalline volume increases as the Mo content increases, according to the XRD curve.

Thermal properties

The DTA traces show the temperature range for crystallization and the glass transition temperature. The DTA curves obtained for all samples are shown in Fig. 5.

Using Fig. 5, calculate T_g (glass transition temperature), T_c (crystallization temperature), and T_m (melting temperature) for the glass characterization temperatures.

Many factors influence the (T_g) characteristic of structural relaxations in the glass network, including bond strength, cross-linking density, and the nature and connectedness of the structural units that make up the network [4].

Table 1 shows that when the amount of MoO₃ increases, the T_g values fall. It can go over the bond dissociation of Bi–O (343 kJ/mol), B–O (806 kJ/mol), and Mo–O (607 kJ/mol) in general. Because the dissociation energy of Mo–O is low, the amount of energy required to break the bond lowers.

The decrease in B–O–B cross-linkages reduces the connectedness of the glass network and results in a looser macromolecular structure with lower internal energy requirements for chain mobility [24].

Increased MoO₃ content, on the other hand, degrades the network structure by increasing voids in the glass matrix. The isolated MoO₄ was not able to form a bond with borate. These are in agreement with the FTIR readings.

Using the characterization temperatures from DTA curves, the thermal stability, capacity of the system to become glass rather than crystal, and glass-forming ability of the system were determined.

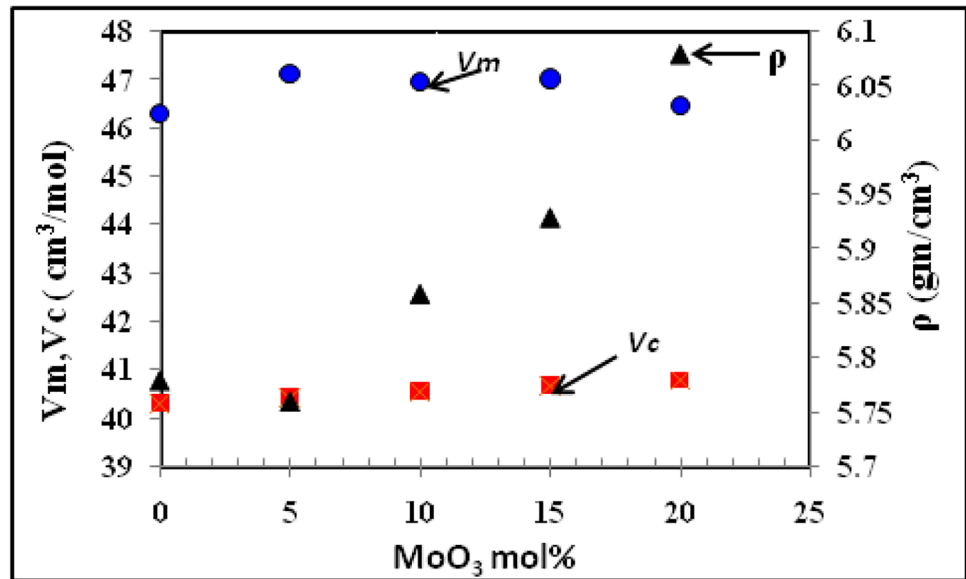
The temperature difference [25] is discovered.

Consider this a useful measure of thermal stability because a higher number suggest a delay in nucleation in the sample.

The results of the samples are listed in Table 1.

It can be seen that glass samples containing 5 and 10 mol% MoO₃ have higher thermal stability than glass samples without MoO₃ and that the value drops as the

Fig. 4 The relation between molar volume, density, and the equivalent crystalline volume as a function of molybdenum content



amount of MoO₃ increases, indicating that the sample is more likely to be a glass crystalline material.

By [26], the Hrub parameter is used to provide information about the sample's potential to become glass or crystalline:

$$H_R = \frac{(T_c - T_g)}{(T_m - T_c)}$$

The results show that when the molybdenum concentration rises, the system becomes more crystalline. The ability to create glass is determined by the following relationship:

$$T_{rg} = T_g/T_m$$

The T_{rg} parameter is utilized to discriminate between homogeneous and heterogeneous nucleation, and the

Fig. 5 DTA curves obtained for all the studied samples

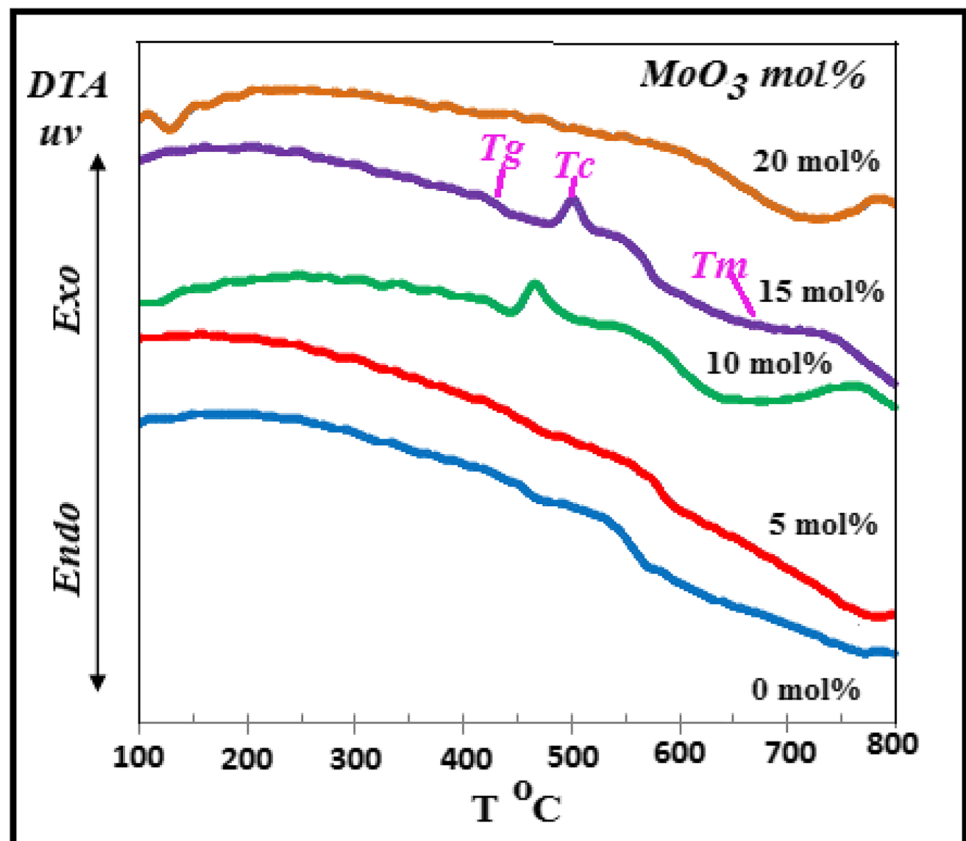
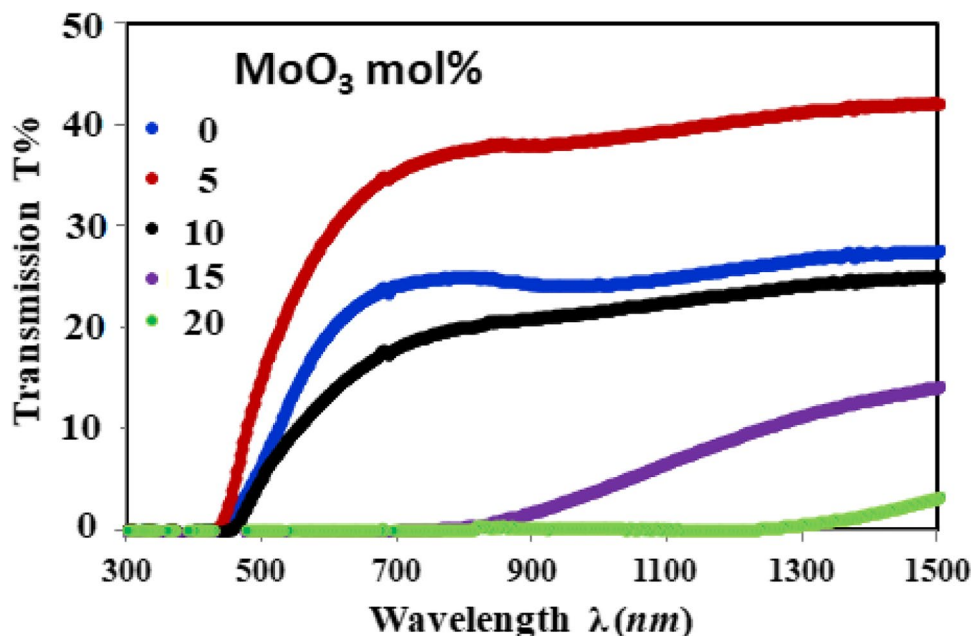


Fig. 6 The typical transmission spectra of glass samples



resultant value is used to calculate the glass-forming ability. The glass has a value in the range of 2/3, which indicates that it has a glass-forming potential. The crystallization surface or volume is indicated by these numbers. This value exceeds 0.58–0.6 surface crystallization but falls short of 0.58–0.6 considerable volume crystallization [25].

The table shows that as the amount of MoO₃ increases, the values fall, indicating that the glass system is prone to volume crystallization.

Optical properties

The UV/Vis/NIR spectra of glass containing various concentrations of MoO₃ are shown in Fig. 6. The curve noticed that the samples in the glass composition act as a sharp-cut filter based on the transmission. The glassy state sample cut light in the near-ultraviolet and visible ranges, but the glass crystalline sample’s cut-off shifted to higher wavelengths. The cut-off wavelength determines the optical band gap, according to the following relationship [11]:

$$E_{ASF}^{opt} = \frac{hc}{\lambda_{cut}} = \frac{1239.38}{\lambda_{cut}}$$

With increasing MoO₃ content, the cut-off wavelength rises higher, breaking the link between the two cations and

forming a distinct BO₃, BO₄ with several configurations, and isolated MoO₄ [27, 28].

With increasing MoO₃ concentration, the optical band gap of the current glass system lowers. As a result, the E_{opt} falls as the number of NBOs grows (the MoO₃ content increases).

According to [29], the refractive index *n* is calculated from the optical band gap:

$$\frac{(n^2 - 1)}{(n^2 + 1)} = 1 - \sqrt{Eg/20}$$

Table 2 shows the results. The linear optical susceptibility X⁽¹⁾ is calculated using the refractive index determined using the following formula:

$$x^{(1)} = (n^2 - 1)/4\pi$$

This equation [30] estimates the third-order nonlinear susceptibility x⁽³⁾ from the value of the linear optical susceptibility X⁽¹⁾:

$$x^{(3)} = [x^{(1)}]^4 \times 10^{-10}$$

Table 2 shows the calculated value of x⁽³⁾, where x⁽³⁾ = (n² - 1)⁴ / 12 (n² represents the nonlinear refractive index)[31].

Table 2 The values of E_{opt} (optical energy gap), refractive index *n*, the linear optical susceptibility X⁽¹⁾, the third-order nonlinear susceptibility x⁽³⁾, and the nonlinear refractive index for all the studied samples

MoO ₃ mol%	λ _{cut} nm	Eg (eV)	Refractive index n	X ⁽³⁾ × 10 ⁻¹³	n ² × 10 ⁻¹²
0	420	3	2.040583	4.02694	7.435871
5	422	2.96	2.049086	4.206917	7.735969
10	440	2.8	2.08452	5.032024	9.095937
15	626	2.1	2.274233	12.17515	20.17207
20	1190	1.05	2.780057	82.3702	111.6419

The third-order nonlinear optical susceptibility is in the range $[(0.38–0.53) 10^{12} \text{esu}]$ based on $X^{(3)}$ values for glass samples free of MoO_3 and containing MoO_3 up to 10 mol%. This indicates that these samples could be used in nonlinear optical applications [32].

Conclusion

Glasses studied utilizing structural (XRD, FTIR), thermal (DTA), XPS, and optical (optical absorption) tests after doping molybdenum into bismuth borate with concentrations ranging from 5 to 20 mol%. The sample with 20 mol% MoO_3 has Bi_2MoO_6 crystalline phase, according to XRD measurements. The steady narrowing of band gaps indicates the creation of non-bridging oxygen and the breaking of BO bonds, resulting in a less rigid glass network. Set up different functional units in FTIR glasses. The study of the Mo 3d XPS spectra indicates the existence of Mo ions in the 6+ oxidation state for the glass compositions. Differential thermal analysis studies demonstrate that the research glasses are thermally stable. Observe a rise in the wavelength of the cut with increased MoO_3 concentration from optical absorption spectra. Nonlinear optical applications are candidates for samples that include MoO_3 up to 10 mol%.

Acknowledgements I. Kashif thanks Prof. Dr. A. M. Sanad for his support throughout my scientific career during his stay with us.

Author contribution The authors equally share in the making of this manuscript.

Data availability The data that support the findings of this study are available from the corresponding author upon reasonable request.

Declarations

Ethics approval This paper meets the ethical standards of this journal.

Consent to participate All authors agree with the review of this paper in this journal.

Competing interests The authors declare that they have no known competing financial interests or personal relationships that could have appeared to influence the work reported in this paper.

All authors states that:

1. This manuscript has not been published, was not, and is not being submitted to any other journal.
2. All necessary permissions for publication were secured prior to submission of the manuscript.
3. All authors listed have made a significant contribution to the research reported and have read and approved the submitted manuscript, and furthermore, all those who made substantive contributions to this work have been included in the author list. All authors have seen and approved the final version of the manuscript being submitted.

The article is the original work, has not received prior publication, and is not under consideration for publication elsewhere.

References

1. Rajyasree, C., Teja, P.M.V., Murthy, K.V.R., Rao, D.K.: Optical and other spectroscopic studies of lead, zinc bismuth borate glasses doped with CuO. *Phys. B Condens. Matter* **406**(23), 4366–4372 (2011)
2. Simon, S., Todea, M.: Spectroscopic study on iron doped silica-bismuthate glasses and glass ceramics. *J. Non. Cryst. Solids* **352**(28–29), 2947–2951 (2006)
3. Venkataraman, B.H., Varma, K.B.R.: Structural and optical properties of $(100-x)(\text{Li}_2\text{B}_4\text{O}_7)_x(\text{SrO}-\text{Bi}_2\text{O}_3-0.7 \text{Nb}_2\text{O}_5-0.3 \text{V}_2\text{O}_5)$ glasses and glass nanocrystal composites. *Opt. Mater.* **28**(12), 1423–1431 (2006)
4. Yadav, A., Dahiya, M.S., Hooda, A., Chand, P., Khasa, S.: Structural influence of mixed transition metal ions on lithium bismuth borate glasses. *Solid. State. Sci.* **70**, 54–65 (2017)
5. Berwal, N., Dhankhar, S., Sharma, P., Kundu, R.S., Punia, R., Kishore, N.: Physical, structural and optical characterization of silicate modified bismuth-borate-tellurite glasses. *J. Mol. Struct.* **1127**, 636–644 (2017)
6. Singh, L., Thakur, V., Punia, R., Kundu, R.S., Singh, A.: Structural and optical properties of barium titanate modified bismuth borate glasses. *Solid. state. Sci.* **37**, 64–71 (2014)
7. Abo-Naf, S.M.: FTIR and UV-VIS optical absorption spectra of gamma-irradiated MoO₃-doped lead borate glasses. *J. Non. Cryst. Solids* **358**(2), 406–413 (2012). <https://doi.org/10.1016/j.jnoncrysol.2011.10.013>
8. Dimitrov, V., Komatsu, T.: Optical basicity and chemical bonding of Bi₂O₃ containing glasses. *J. Non. Cryst. Solids* **382**, 18–23 (2013)
9. Shaaban, K.H.S., Abo-Naf, S.M., AbdElnaeim, A.M., Hassouna, M.E.M.: Studying effect of MoO₃ on elastic and crystallization behavior of lithium diborate glasses. *Appl. Phys. A* **123**(6), 1–9 (2017)
10. Shaaban, K.H.S., Saddeek, Y.B.: Effect of MoO₃ content on structural, thermal, mechanical and optical properties of (B₂O₃-SiO₂-Bi₂O₃-Na₂O-Fe₂O₃) glass system. *SILICON* **9**(5), 785–793 (2017)
11. Ali, A.A., Rammah, Y.S., El-Mallawany, R., Souri, D.: FTIR and UV spectra of pentatertiary borate glasses. *Measurement* **105**, 72–77 (2017)
12. Moustafa, E., Saddeek, Y.B., Shaaban, E.R.: Structural and optical properties of lithium borobismuthate glasses. *J. Phys. Chem. Solids* **69**(9), 2281–2287 (2008)
13. Bajaj, A., Khanna, A., Chen, B., Longstaffe, J.G., Zwanziger, U., Zwanziger, J.W., Gómez, Y., González, F.: Structural investigation of bismuth borate glasses and crystalline phases. *J. Non. Cryst. Solids* **355**(1), 45–53 (2009)
14. Peng, Y., Zhang, Y., Tian, F., Zhang, J., Yu, J.: Structure tuning of Bi₂MoO₆ and their enhanced visible light photocatalytic performances. *Crit. Rev. Solid State Mater. Sci.* **42**(5), 347–372 (2017)
15. Rejisha, S.R., Anjana, P.S., Gopakumar, N., Santha, N.: Synthesis and characterization of strontium and barium bismuth borate glass-ceramics. *J. Non. Cryst. Solids* **388**, 68–74 (2014)
16. Boda, R., Shareefuddin, M., Chary, M.N., Sayanna, R.: FTIR and optical properties of europium doped lithium zinc bismuth borate glasses. *Mater. Today Proc.* **3**(6), 1914–1922 (2016). <https://doi.org/10.1016/j.matpr.2016.04.092>

17. Mekki, A., Khattak, G.D., Wenger, L.E.: structural and magnetic properties of MoO₃–TeO₂ glasses. *J. Non-Cryst. Solids*. **351**, 2493–2500 (2005)
18. Pal, M., Hirota, K., Tsujigami, Y., Sakata, H.: Structural and electrical properties of MoO₃–TeO₂ glasses. *J. Phys. D. Appl. Phys.* **34**, 459–464 (2001)
19. Lakshminarayana, G., Baki, S.O., Lira, A., Sayyed, M.I., Kityk, I.V., Halimah, M.K., Mahdi, M.A.: X-ray photoelectron spectroscopy (XPS) and radiation shielding parameters investigations for zinc molybdenum borotellurite glasses containing different network modifiers. *J. Mater. Sci* **52**, 7394–7414 (2017)
20. Pascuta, P., Pop, L., Rada, S., Bosca, M., Culea, E.: The local structure of bismuth borate glasses doped with europium ions evidenced by FT-IR spectroscopy. *J. Mater. Sci. Mater. Electron.* **19**(5), 424–428 (2008)
21. Berkemeier, F., Voss, S., Imre, Á.W., Mehrer, H.: Molar volume, glass-transition temperature, and ionic conductivity of Na- and Rb-borate glasses in comparison with mixed Na–Rb borate glasses. *J. Non. Cryst. Solids* **351**(52–54), 3816–3825 (2005)
22. Ramteke, D.D., Gedam, R.S.: Luminescence properties of Gd³⁺ containing glasses for ultra-violet (UV) light. *J. Rare Earths* **32**(5), 389–393 (2014)
23. Berwal, N., Kundu, R.S., Nanda, K., Punia, R., Kishore, N.: Physical, structural and optical characterizations of borate modified bismuth–silicate–tellurite glasses. *J. Mol. Struct.* **1097**, 37–44 (2015)
24. Rani, S., Sanghi, S., Ahlawat, N., Agarwal, A.: Influence of Bi₂O₃ on thermal, structural and dielectric properties of lithium zinc bismuth borate glasses. *J. Alloys Compd.* **597**, 110–118 (2014)
25. Atyia, H.E., Farid, A.S.: Non-isothermal crystallization kinetics of ternary Se₉₀Te₁₀-xPbx glasses. *J. Cryst. Growth* **436**, 125–133 (2016)
26. Mhareb, M.H.A., Hashim, S., Ghoshal, S.K., Alajerami, Y.S.M., Bqoor, M.J., Hamdan, A.I., Saleh, M.A., AbdulKarim, M.K.B.: Effect of Dy₂O₃ impurities on the physical, optical and thermoluminescence properties of lithium borate glass. *J. Lumin.* **177**, 366–372 (2016)
27. Kim, N.J., La, Y.H., Im, S.H., Han, W.-T., Ryu, B.K.: Effect of ZnO on physical and optical properties of bismuth borate glasses. *Electron. Mater. Lett.* **5**(4), 209–212 (2009)
28. Rejisha, S.R., Anjana, P.S., Gopakumar, N.: Effect of cerium (IV) oxide on the optical and dielectric properties of strontium bismuth borate glasses. *J. Mater. Sci. Mater. Electron.* **27**(5), 5475–5482 (2016)
29. Kashif, I., Ratep, A., Adel, G.: Polarizability, optical basicity and optical properties of SiO₂B₂O₃Bi₂O₃TeO₂ glass system. *Appl. Phys. A* **124**(7), 1–9 (2018)
30. Tashera, T., Dimitrov, V.: Optical properties and structure of B₂O₃BaOV₂O₅ Glasses. *J. Chem. Technol. Metall.* **50**, 441 (2015)
31. Vogel, E.M., Weber, M.J., Krol, D.M.: Nonlinear optical phenomena in glass. *Phys. Chem. Glass.* **32**, 231–254 (1991)
32. Rao, L.S., Thirimal, C., Rao, P.R.: Dielectric dispersion, linear and nonlinear optical properties of Li₂O–WO₃–B₂O₃: V₂O₅ glasses. *J. Adv. Dielectr.* **10**(3), 2050006 (2020)

Publisher's note Springer Nature remains neutral with regard to jurisdictional claims in published maps and institutional affiliations.